Motor Proteins

Charles L. Asbury[1,3] *and Steven M. Block*[1,2]
[1] *Department of Biological Sciences, Stanford University, Stanford, California, USA*
[2] *Department of Applied Physics, Stanford University, Stanford, California, USA*
[3] *Present Address: Department of Physiology and Biophysics, University of Washington, Seattle, Washington, SA*

Encyclopedia of Molecular Cell Biology and Molecular Medicine, 2nd Edition. Volume 8
Edited by Robert A. Meyers.

ISBN: 3-527-30550-5

Keywords

Allostery
Pertaining to or involving a change in conformation caused by the attachment of a ligand or substrate.

Mechanoenzyme
A catalytic enzyme that produces motion and force.

Processivity
A measure of the number of catalytic cycles an enzyme undergoes before detaching from the substrate. In the context of motors, processivity is proportional to the average distance over which the enzyme translocates on its filamentous substrate before detaching.

Substrate
A molecule on which an enzyme acts. In the context of molecular motors, either the fuel source (e.g. NTPs), or the force-generating partner (e.g. actin filament).

Working Stroke
A conformational change that occurs during a single round of catalysis, and which drives motion and force production. The working stroke length, or working distance, is the maximal distance associated with the stroke. The working distance can be different from the distance between consecutive attachment sites on the partner filament.

Cellular motions have fascinated biologists during the 400 years since the invention of the optical microscope first allowed them to be seen. Today, we know that motions underlying the most essential processes of life – such as cell division, energy transduction, muscle contraction, DNA replication, transcription, and translation – are generated by molecular motors. A molecular motor is a protein, or a complex of proteins and nucleic acids, that produces motion and force. For fuel,

many molecular motors consume nucleotide triphosphates, breaking an energy-rich phosphate bond to release chemical energy, and then converting this into mechanical work. Other motors tap electrochemical gradients that exist across membranes within bacteria, mitochondria, and chloroplasts. Motor proteins are Nature's nanomachines, and they often function with efficiency that far exceeds the best human-engineered machines.

1 Introduction

Producing motion and force is the primary role of the "classic" molecular motors, myosin, kinesin, and dynein. These *mechanoenzymes* all hydrolyze ATP as a source of energy and drive motion along protein filaments. Myosin generates motion along filamentous actin, and is well known for its role in muscle contraction. The seemingly simple act of flexing ones arm requires $\sim 10^{17}$ myosins working together to slide $\sim 10^{15}$ actin filaments toward one another. Kinesin and dynein move along microtubule filaments. An essential role of kinesin is to haul vesicles across neurons. This can be a 6-day haul since the longest neurons are more than a meter, and vesicle transport proceeds at only 2 $\mu m\ s^{-1}$. Dynein causes the beating of flagella and cilia, such as those lining the lungs, by sliding microtubules past one another.

Besides the classic motors, there are many "nontraditional" motor proteins. In some cases, motion and force production are byproducts rather than a primary function. The main role of DNA and RNA polymerases is to copy and transcribe the genetic code. In order to do so, they move along their nucleic acid templates, sometimes with amazing endurance. A single RNA polymerase molecule can transcribe all 2.5 million bases of the human dystrophin gene in 14 h, at roughly 50 bases per second. Another nontraditional motor is F_1F_0-ATP synthase, which is responsible for replenishing the entire pool of ATP in all cells using energy derived from metabolism. As this enzyme toils, it also spins – it is a rotary motor. A flow of protons causes a shaft within the motor to rotate continuously, and shaft rotation is then coupled to the synthesis of ATP from ADP and phosphate. A third type of nontraditional motor activity is driven by the cytoskeletal polymers, actin, and tubulin. In addition to their roles as structural cables and girders for maintaining cell shape, and as highways for motor proteins to move along, these polymers are themselves dynamic machines that produce force. The leading edges of macrophages and other crawling cells are pushed outward by polymerizing actin filaments. Microtubule depolymerization generates tension that pulls chromosomes apart prior to cell division.

This chapter is a survey of the main classes of molecular motors. It begins with a discussion of the classic mechanoenzymes, myosin, kinesin, and dynein. These motors have been the subject of biophysical research for decades, and our understanding of their function serves as a foundation for the study of other motors. The chapter then turns to nontraditional motors, focusing on a handful of key examples, including nucleic acid enzymes (RNA polymerase), rotary motors

(F_1F_0-ATP synthase, and the bacterial flagellar motor), and protein polymers (actin and tubulin). A central goal of research on motor proteins is to determine how underlying biochemical events, such as ATP hydrolysis, are coupled to mechanical action. Progress toward this goal is chronicled throughout the chapter through description of experiments with classic and nontraditional motors.

2 Classic Molecular Motors

Myosin, kinesin, and dynein are founding members of large families of proteins whose primary function is to generate motion and force. Owing to their structural resemblance, the motors of each family operate in a manner similar to the founding proteins. However, they drive a wide variety of different cellular motions beyond the stereotypical roles of muscle contraction, vesicle transport, and the beating of cilia. There are at least 15 classes of myosin (traditionally denoted with roman numerals I through XV), and only a handful are involved in muscle contraction. Some of the other types are implicated in vesicle budding, cytokinesis, and organelle transport along actin cables. Likewise, kinesin-like proteins and cytoplasmic dyneins are essential for the formation and positioning of the mitotic spindle, chromosome separation prior to cell division, and organelle

Fig. 1 Structures of some classic and nontraditional molecular motors. (a) Muscle myosin consists of two heads connected to a common coiled-coil tail. The heads bind actin and carry ATP hydrolysis activity. A rodlike portion of each head (light gray) functions as a lever-arm, tilting ~70° relative to the remainder of the head (dark gray) upon attachment to an actin filament. The tail promotes bundling of myosin molecules into thick filaments. (b) Kinesin also has two heads, connected through short polypeptides called *neck linkers* to a common coiled-coil stalk. The heads bind microtubules and carry ATP hydrolysis activity. A conformational change of the neck linkers may drive kinesin motion. The tail binds cargo. (c) Each dynein molecule consists of a donut-shaped head with two rodlike structures, the stem and stalk, emanating from the head. The head contains four ATP-binding sites, only one of which is catalytically active. The tip of the stalk binds microtubules. To drive motion, the head and stalk rotate relative to the stem, which attaches to cargo and can also bundle two or three dynein heads together. (d) RNAP is shaped like a claw, which opens to allow a DNA template to enter, and then wraps completely around the DNA during transcription. While transcribing, RNAP separates a portion of the DNA duplex called the *transcription bubble*, and maintains registration of a short section of hybrid RNA:DNA duplex. Nucleotides enter through a channel, leading to the active site, where they are incorporated into the nascent mRNA chain. (e) F_1F_0-ATP synthase consists of two rotary motors, connected to a common shaft, which act as a motor-generator pair. The F_0 portion taps a proton gradient across the inner mitochondrial membrane to drive spinning of the rotor (c_{12}) relative to the stator (ab_2). The F_1 portion sits directly above F_0, and contains a shaft ($\gamma\varepsilon$) that is rigidly fixed to the rotor of F_0, and also a ring $(\alpha\beta)_3$ that is rigidly fixed to the stator of F_0. Spinning of the shaft relative to the ring drives ATP synthesis. The isolated F_1 portion is known as F_1-ATPase because in the presence of ATP it will spin in reverse, catalyzing ATP hydrolysis. (e) Cross-sectional view of the rotary motor of bacterial flagella. The motor core contains a stack of rings (rotor), embedded in the multilayered cell wall that rotates as a single unit about an axis (dashed line) perpendicular to the surface of the bacteria. Rotation is driven by torque-generating units composed of MotA and MotB proteins. The MotA/B complex is anchored to fixed structures (peptidoglycan) within the cell wall. Protons flow through a channel within MotA/B, where protonation and deprotonation of MotB induces conformational changes in MotA, which attaches and detaches from the base of the rotor and drives its rotation.

movement along microtubules. The discussion here centers on the founding proteins, their functional properties, and some of the experiments that uncovered these properties. Particular attention is given to *in vitro* work with single motor molecules.

2.1 Muscle Myosin: Tilting Cross-bridges Drive Contraction

The motor activity of myosin was discovered more than 50 years ago. Electron microscopy revealed that muscle fibers consist of parallel thick and thin filaments that slide past one another during contraction. Tiny structures termed "cross-bridges," connecting laterally between the filaments, were suspected to drive filament sliding. In some images, the cross-bridges projected from the thick filaments at right angles, but in others, they were tilted, depending on tissue preparation conditions. These observations led to the theory, now well established, that cross-bridges drive filament sliding by cyclically attaching to the thin filaments, tilting, detaching, and untilting.

The thick filaments are now known to be bundles of myosin molecules. Each myosin consists of two identical 200-kDa polypeptides, plus two pairs of light chains (20 kDa). The heavy chains fold into twin globular heads connected to a common coiled-coil tail (Fig. 1a). Two light chains bind each head near the head–tail junction. Myosins bundle together by their long tails, and their heads project from the bundles, forming the cross-bridges that drive

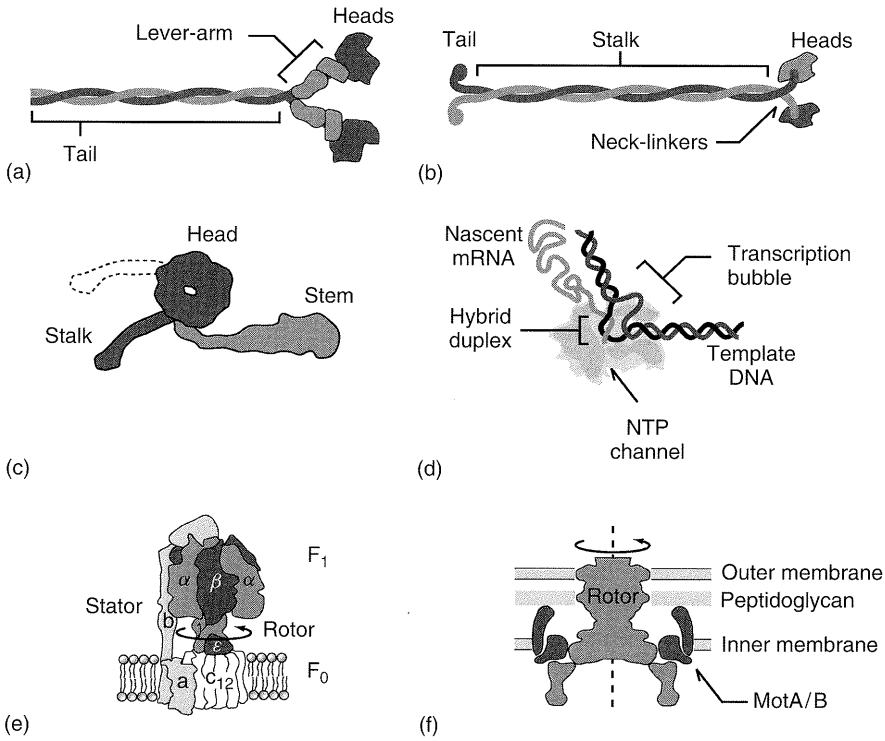

filament sliding. The heads can bind and hydrolyze ATP, and also carry a site that attaches to actin, the main component of the thin filaments, with ATP-dependent affinity. In high-resolution structures, a rodlike portion of the myosin head is found in several different orientations relative to the remainder of the head. Tilting of this "lever-arm," not the entire head, probably drives filament sliding.

The thin filaments of muscle are composed mainly of actin. Actin is a roughly spherical protein that polymerizes into a ropelike structure, with two strands, called *protofilaments*, that twist around one another. The filaments are polar, with a "plus" or "barbed" end, and a "minus" or "pointed" end, which are structurally different. During muscle contraction, the thick filaments slide toward the plus ends of the thin filaments.

2.2 Seeing is Believing: Motility Assays Demonstrate Motor Activity

A wealth of biochemical and structural information supports the tilting cross-bridge model of muscle contraction. However, the most compelling evidence for myosin motility comes from direct observation of motion generated *in vitro*. Myosin and actin are too small to see in an optical microscope. So, *in vitro* motility assays depend on various labeling schemes to render the motion visible. In the earliest assays, micron-sized beads were coated with myosin, and the beads were then observed to move along actin cables in the cytoplasm of the alga *Nitella*, and later along purified actin filaments bound to a glass surface. In an alternate strategy, actin filaments were made visible by fluorescent labeling, and gliding of these labeled filaments on myosin-coated glass surfaces was observed in a fluorescence microscope (Fig. 2a). These important experiments established beyond doubt that actin and myosin alone, without any additional components from muscle cells, were sufficient to generate motion and force. Consistent with the rotating cross-bridge theory, ATP was required for the motility, and the myosins moved toward the plus ends of the actin filaments. Filaments glided *in vitro* at 6000 nm s^{-1} (Table 1), similar to the speed at which thick and thin filaments slide past one another during muscle contraction. As discussed below, these two basic tests – the "bead assay" and the "gliding filament assay" – have been adapted and refined to study a variety of other motors in addition to myosin (Fig. 2b through d).

2.3 Kinesin: Intracellular Porter

Motility assays were instrumental in the discovery of kinesin. Observations of the squid giant axon suggested the existence of motors that consume ATP and haul vesicles at speeds of 1 to 2 μm s^{-1} along the dense array of microtubule filaments within the axon. A putative motor was first isolated by locking the vesicles onto the microtubules using a nonhydrolyzable ATP analog, AMPPNP, followed by purification of the microtubules, and then release of the motor with ATP. A gliding filament assay identical to that developed for myosin confirmed that the purified protein, kinesin, was indeed a motor: glass surfaces coated with kinesin supported the ATP-dependent gliding of microtubules. The gliding velocity, 800 nm s^{-1} (Table 1), closely matched the speed of vesicle transport.

Additional assays, using microtubules marked to reveal their intrinsic polarity, revealed the direction of kinesin-driven

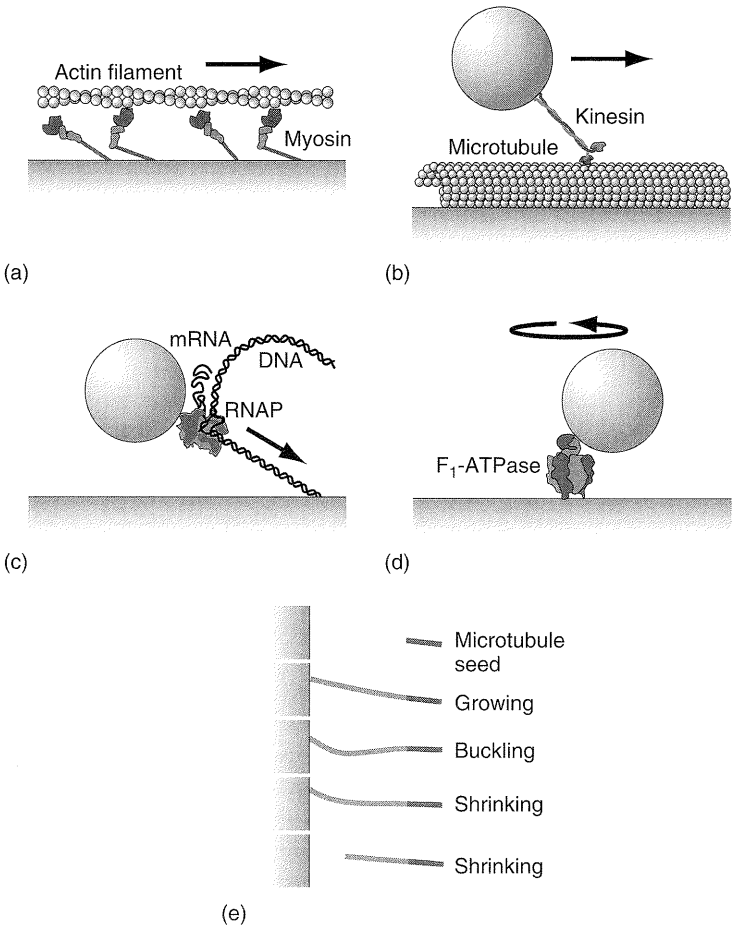

Fig. 2 Motility assays adapted for various molecular motors. (a) In the gliding filament assay, coverslip-bound motors drive filaments to move in a direction parallel to the filament long axis. Here, many myosin heads are shown interacting with a single actin filament. (b) In the bead motility assay, motors are attached to microscopic glass or plastic beads, which are pulled by the motors along coverslip-bound filaments. Kinesin is shown moving along a microtubule. (c) The tethered particle assay was developed to study the motion of nucleic acid enzymes along DNA filaments. Here, a microscopic bead is attached to RNA polymerase, which is transcribing a DNA filament that is attached at one end to the coverslip. Transcription results in a shortening (or lengthening) of the tether (depending on which end of the DNA is surface-bound). (d) In the rotation assay for F_1-ATPase, the motor is attached to a coverslip, and the orientation of the shaft is marked by off-axis attachment of a microscopic bead or filament. Spinning of the shaft causes the bead or filament to rotate. (e) Force generation by polymerization has been demonstrated by growing dynamic microtubule extensions from coverslip-bound seeds. The microtubules continue to elongate even after their growing ends encounter a barricade, which generates enough compressive force to buckle the filaments.

Tab. 1 Properties of selected molecular motors.

Protein Machine	*Molecular Weight (kDa)*	*Force-generating Partner*	*Energy Source*	*Maximum Speed (nm s^{-1})*[a]	*Maximum Force (pN)*[a]	*Step Size (nm)*[a]	*Processivity (cycles)*
Kinesin, native heterotetramer	340	Microtubule	ATP	1800			
Kinesin, truncated active homodimer	90	Microtubule	ATP	800	6	8	100
Myosin II, native heterohexamer	500	Actin filament	ATP	6000	1.5		
Myosin II, active HMM fragment	110	Actin filament	ATP	8000		6	1
Dynein, inner arm subspecies c	500	Microtubule	ATP	700	1.1	$8n$ ($n = 1, 2, 3 \ldots$)	~10
RNA polymerase, *E. coli* core enzyme	380	dsDNA	NTPs	5	27	0.34	>10 000
F_1F_0-ATP synthase	540	n/a	Protonmotive				n/a
F_1-ATPase, active rotary motor	350	n/a	ATP	150 Hz	40 pN nm	120°	n/a
Bacterial flagellar motor, basal body	9500	n/a	Protonmotive	300 Hz	4600 pN nm		n/a
Microtubule, growing	110 (tubulin dimer)	n/a	Binding	~50	4		n/a
Microtubule, depolymerizing		n/a	GTP	~500			
Actin filament, growing	40 (G-actin monomer)	n/a	Binding	~15			n/a

[a] Different units apply to the rotary motors, F_1F_0-ATP synthase, F_1-ATPase, and the bacterial flagellar motor. For these, the maximum rotation rate, torque, and angular step size are reported in units of Hz, pN nm, and degrees, as noted.

motion. Microtubules are rigid, tube-shaped polymers, composed of tubulin proteins arranged in a lattice, resembling a miniature drinking straw. Like actin filaments, microtubules have two structurally distinct ends, called "plus" and "minus". Polarity-marked filaments driven by kinesin glided with their minus ends leading, implying that kinesin was moving toward the plus ends.

Kinesin and myosin share many structural and functional similarities. Like myosin, each kinesin molecule consists of two identical polypeptides that form twin heads connected to a common coiled-coil stalk (Fig. 1b). The motor activity is carried by the heads. Each head hydrolyzes ATP and attaches to microtubule filaments with nucleotide-dependent affinity. But unlike myosin, the tail of kinesin does not cause bundling, it binds the motor to its cargo. Furthermore, atomic structures of kinesin heads are devoid of any rodlike structure resembling the lever-arm of myosin. Lacking a lever, kinesin's working stroke is likely to be very different from that of myosin.

2.4 Ciliary Dynein: The Dark Horse

Comparatively little functional information is available for the third classic motor, dynein, even though its activity was discovered around the same time as that of myosin. Electron micrographs revealed lateral connections between the parallel microtubules in cilia and flagella, similar to the myosin cross-bridges in muscle. The cross-bridges in cilia and flagella are dynein motors that drive bending motions by sliding microtubules past one another.

Dynein is larger and structurally more complex than kinesin or myosin, but it has many features common to all the classic motors. Depending on the source, dynein consists of one, two, or three large (500 kDa) polypeptides. Each of these forms a donut-shaped head, with two rodlike structures emanating from it, the "stem" and the "stalk" (Fig. 1c). The stem functions similar to the tails of kinesin and myosin, bundling the heads together, and also anchoring them tightly to their cargo. The tip of the stalk binds microtubules in an ATP-dependent manner, like the microtubule binding site within each of kinesin's heads. No atomic resolution structures are available for dynein, but electron microscopy of single dynein particles revealed a conformational change akin to the lever-arm tilting of myosin: under different nucleotide conditions, the stem adopts two different orientations relative to the head and stalk. Thus, dynein may move its stem-bound cargo by cyclically attaching via the stalk to a microtubule, rotating the stalk and head, detaching from the microtubule, and then unrotating. Dynein supports microtubule gliding and bead motion in *in vitro* assays. The direction of dynein-driven motion is toward the minus end of the microtubule, opposite that of kinesin-driven motion.

Dynein's complex structure contains a number of features with unknown functional significance. Dynein motors from different sources have different numbers of heads. Each donut-shaped head consists of six different subdomains arranged in a hexameric ring. Four of these subdomains bind ATP, but only one catalyzes hydrolysis. Nucleotide binding, but not hydrolysis, at one of the other subdomains is essential for motor activity. Uncovering the reasons for this complexity and elucidating dynein's mechanism of action are important frontiers for future research.

2.5 Processivity Allows Kinesin to Work Alone

Soon after its discovery, kinesin was found to possess a tenacity that set it apart from myosin and dynein. Kinesin is highly *processive*, staying attached to the microtubule as it undergoes many catalytic cycles, and translocating over relatively long distances before detaching. This processivity was first demonstrated when gliding filaments or moving beads were found to move long distances (1–2 μm), even when the surface density of motors on the slide or bead was extremely low, ensuring that single kinesin–microtubule interactions were very likely. Several independent lines of evidence now provide very strong evidence of kinesin's processivity (see Fig. 3).

The processivity of kinesin probably evolved as a means to conserve cellular resources. Kinesin's role of transporting vesicles across neurons is a critical task that must be accomplished repeatedly and with high reliability in order for these cells to function. The longest neurons contain millions of vesicles that each take weeks to make the journey from one end to the other. Kinesin's high processivity allows this Herculean task to be completed by just a few motors bound to each vesicle. In principle, the job could also be accomplished by nonprocessive motors, but many more motors would be required. The cell, in turn, would have to devote more energy and resources into producing these additional molecules.

Apart from its biological significance, kinesin's processivity has been a great advantage for experimentalists, allowing the first studies of single motor molecules. Motility assays for myosin relied on hundreds of motors acting together because the tiny tilting motions, or *working strokes*, of the individual heads are too small to see in a conventional optical microscope. However, owing to their high degree of processivity, kinesins generate hundreds of working strokes during each encounter with a microtubule moving distances of ~1 μm. The summation of many strokes renders the motion of individual kinesin motors easily visible.

Results from single molecule motility assays revealed a number of insights about how kinesin moves. The motion of kinesin-driven beads *in vitro* was not random over the microtubule surface, but appeared to follow a path parallel to the protofilaments. Gliding filament assays supplied strong evidence for protofilament tracking, when abnormal microtubules with helical protofilaments were shown to rotate about their long axis as they moved. In bead assays, engineered kinesin proteins with only one head failed to generate highly processive motion, indicating that two heads are, in fact, better than one.

2.6 Rowers Versus Porters: Duty Ratio Makes a Difference

The head domains of myosin and kinesin differ markedly in their duty ratio, the fraction of time during each biochemical cycle that they remain attached to their partner filament. Myosin possesses a low duty ratio that allows groups of molecules to work together efficiently, like the rowers of a large canoe, while kinesin has a high ratio, befitting its role as a lone porter. A myosin head has high affinity for actin just after hydrolysis, when the nucleotide-binding pocket contains either ADP and phosphate, or ADP alone, and low affinity when the pocket is empty or contains ATP. The timing of transitions between these states ensures that the high-affinity

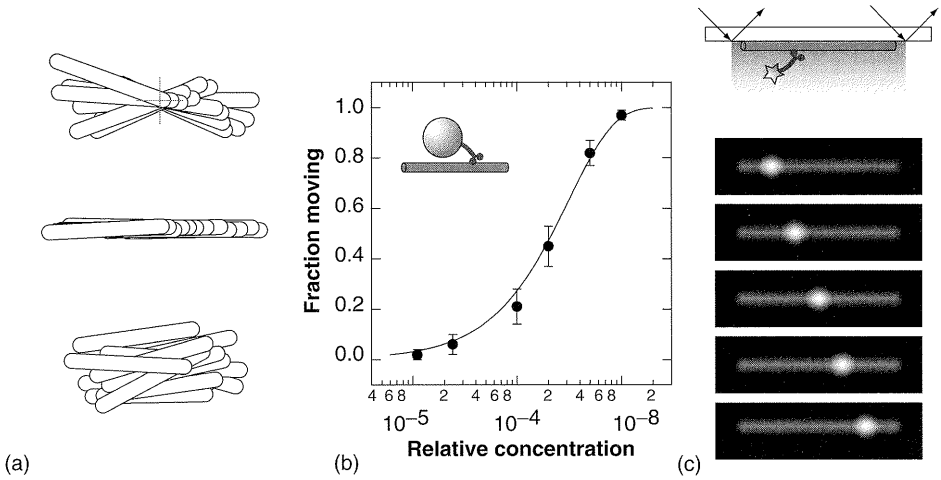

Fig. 3 Strong evidence for the processivity of kinesin. The first evidence for processivity was that kinesin-driven motion persisted *in vitro* even when the surface density of motors was extremely low. (a) Nodal point pivoting in the gliding filament assay also indicated processivity. Microtubules gliding on surfaces decorated sparsely with kinesin rotated erratically about a fixed location, even as they moved through this nodal point. When the trailing end of the microtubule reached the nodal point, it dissociated from the surface and diffused back into solution. A single motor at the nodal point presumably drove the motion (top). Negligible rotation occurred at high motor densities, when multiple motor–filament interactions constrained the filament orientation (middle). Both types of motion were distinct from thermal motion of free filaments in the absence of motor (bottom). [Adapted from Howard, J., Hudspeth, A.J., Vale, R.D. (1989) Movement of microtubules by single kinesin molecules, *Nature* **342**, 154–158.] (b) In the kinesin bead assay, the fraction of moving beads, f, decreased gradually as the relative motor concentration, C, was lowered, as expected if one molecule is sufficient to produce movement. The curve shows a one parameter (λ) fit to Poisson statistics, $f = 1 - \exp(-\lambda C)$. [Adapted from Svoboda, K., Block, S.M. (1994) Force and velocity measured for single kinesin molecules, *Cell* **77**, 773–784.] In the low-density regime, moving beads continued to translocate at normal speeds over distances that were independent of motor concentration (data not shown). (c) A third method used a microscope capable of imaging single fluorophores bound to kinesin (upper panel). The movement of labeled motors along coverslip-bound filaments was directly observed (shown schematically in the lower five panels). [Adapted from Vale, R.D., Funatsu, T., Pierce, D.W., Romberg, L., Harada, Y., Yanagida, T. (1996) Direct observation of single kinesin molecules moving along microtubules, *Nature* **380**, 451–453.] Labeling the motor by fusion to green fluorescent protein avoided chemical modification with reactive dyes, which can damage the motors, and ensured that every motor was labeled with the same number of fluorophores.

states represent <2% of the total cycle time. This low duty ratio is an adaptation that allows the myosin heads to avoid interfering with each other when many are acting on the same actin filament. They detach very quickly after undergoing a working stroke, so the speed of filament sliding is not limited by the hydrolysis rate of the individual heads. In contrast, kinesin heads have a duty ratio >50%, which partially explains the processivity of the motor. Even if the cycles of the two heads were completely uncorrelated, their high duty ratio would ensure that, on

average, at least one was always bound to the microtubule.

2.7 Molecular Tug-of-war: Applying Force to Individual Motors

With the development of single molecule assays, it became possible to directly measure the forces generated by individual motors. One method for measuring force production by kinesin was to attach a microtubule filament to a flexible glass fiber, and then hold the fiber near a surface sparsely coated with kinesin. As individual kinesins on the surface bound and moved along the microtubule, they pulled against the glass fiber and caused it to bend. By measuring the amount of bending, the maximum force against which a kinesin motor could move was estimated to be 5 or 6 pN.

Another method for applying force to individual kinesin molecules, which gave a similar estimate of the stall force and also led to a number of other discoveries, was to use an optical trap. An optical trap is made by focusing a laser through the objective lens of a high-magnification microscope, creating a very bright light spot at the specimen. The focused light traps small objects such as micron-sized beads. When the trapped object is moved away from the center of focus, it feels a restoring force pulling it back that is proportional to the distance from the center, as if the trap was a stretched spring pulling on the object. To apply force to kinesin, an optical trap was used to grab beads with single kinesin molecules attached, and to place them near microtubules stuck onto to a glass surface. When the kinesin began moving along the microtubule, it pulled the bead from the trap center, and the trap supplied a restoring force that placed tension on the kinesin. As the bead was pulled gradually away from the trap center, the force increased and the motor speed decreased, halting when the force reached 6 pN.

2.8 Motors Move in Discrete Steps

Kinesin molecules move discontinuously over the microtubule surface, advancing in discrete 8-nm increments and dwelling at well-defined positions between advancements (Fig. 4). Two key innovations allowed the first observation of steps in the motion of kinesin-driven beads. First, tension supplied by an optical trap suppressed the random, thermally driven ("Brownian") motion that would otherwise dominate. Second, the bead position was measured with very high spatial and temporal resolution by monitoring the distribution of scattered light with a photodetector. The 8-nm step size (Fig. 4b) matches the spacing of tubulin dimers in the microtubule lattice. Similar experiments with dynein, which is processive under some conditions, suggest that it also moves stepwise, advancing by multiples of 8 nm.

Optical trapping has been applied to measure the motion of single myosin motors. A different technique than that used for kinesin was required because the interactions between a myosin molecule and an actin filament are fleeting, lasting only a few tens of milliseconds. To resolve these quick attachments, an assay was developed in which an actin filament with beads attached at both ends was suspended between two optical traps and held near a surface sparsely coated with myosin (Fig. 4c). Thermal motion of the beads decreased when a motor became attached to the filament, and the average position of the beads shifted abruptly, due to the tilting of the myosin head, by 6 nm. This tiny

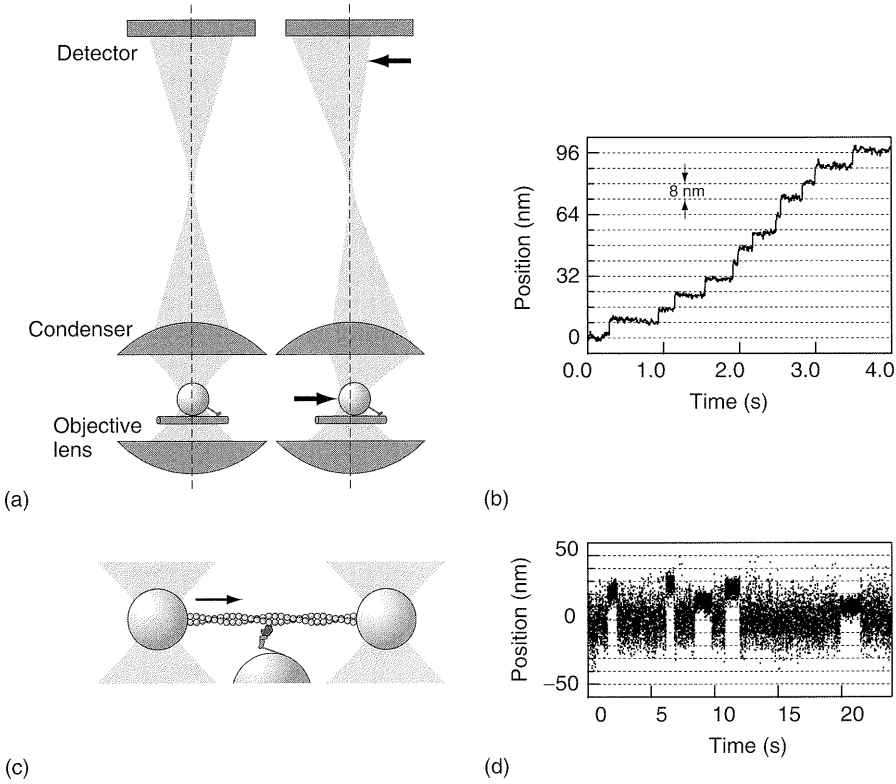

Fig. 4 Measuring the discrete motions of kinesin and myosin molecules using optical traps. Both methods use microscopic beads as handles to apply force, and as markers for the position of the motor or filament. (a) An optical trap applies tension during kinesin-driven movement of a bead along a coverslip-bound microtubule, and this tension reduces thermal motion of the bead so that individual 8-nm steps can be resolved. Bead position is detected with very high spatial resolution by monitoring the distribution of scattered light with a photodetector. (b) Example trace showing 8-nm steps generated by a single kinesin molecule. (c) The three-bead assay developed for measuring working strokes of muscle myosin. An actin filament is pulled taut between two microscopic beads held in optical traps. Binding of a single myosin head to the filament reduces thermal motion of the beads, and also induces a working stroke in the myosin, which causes the beads to deflect by 5 to 15 nm. (d) Example trace showing interactions between a single myosin head and an actin filament. [Data reprinted with permission from Lister, I., Schmitz, S., Walker, M., Trinick, J., Buss, F., Veigel, C., Kendrick-Jones, J. (2004) A monomeric myosin VI with a large working stroke, *EMBO J.* **23**, 1729–1738.]

distance is the maximum sliding distance that a myosin molecule can generate during a single interaction with actin during muscle contraction. More than a million of these interactions are evidently required just to lift a finger.

2.9 Different Strokes: Variation Within and Across Motor Families

In accordance with their diverse roles, motors of the myosin, kinesin, and dynein

families often have important differences in the way they move. The cellular role of type V myosin, for example, is more similar to that of kinesin than to muscle myosin. Myosin V acts alone or in small numbers to transport vesicles and organelles along actin cables. It was therefore not surprising to find that this myosin, like kinesin, exhibits processive movement, taking several steps along an actin filament before detaching. The step size of myosin V, 36 nm, is much larger than that of kinesin, and matches the wide spacing of binding sites that occur every half-period in the actin helix. The structure of myosin V explains how it can generate such large movements. Each head contains a lever-arm that is 24 nm long, three times longer than the lever-arm of muscle myosin.

Diversity within motor families invites comparison, which can illuminate important aspects of motor function. Strong evidence supporting the tilting lever-arm model came from comparisons of gliding speeds and stroke lengths generated *in vitro* by myosin-family motors with different lever-arm lengths. The speeds and stroke lengths varied in proportion with the lever-arm length, as predicted by the model. Structural differences between kinesin and Ncd, a related motor that moves toward the opposite end of microtubules, suggested that a "gearbox" region just outside the head domain controls the direction of motion of these motors. This hypothesis was confirmed by testing chimeric motors, made by swapping the gearbox regions of the two proteins, in gliding filament assays.

2.10
Fuel Economy and Energy Efficiency

How many ATP molecules does a motor require to generate a working stroke or step? Is this "fuel economy" always the same? For kinesin, the coupling ratio – the number of ATPs consumed per step – has been measured by comparing the stepping rate in single molecule assays to the rate of ATP hydrolysis. Over a wide range of ATP concentrations and loads, one ATP is hydrolyzed per 8-nm step. This tight, 1 : 1 coupling implies that the energy efficiency of kinesin can be very high. ATP hydrolysis under physiological conditions is worth ~80 pN nm (or $2 \cdot 10^{-23}$ kcal). When kinesin generates 8-nm steps under 5 pN of load, it produces as much as 40 pN nm (10^{-23} kcal), or 50% of the total chemical energy available. So kinesin is more than twice as efficient as the best man-made gasoline engines, which are 24% efficient at full power, and typically achieve only 10 to 15% on the road.

The energy efficiency of cytoplasmic dynein, 10%, is considerably lower than that of kinesin. However, dynein's complex structure may act like an automobile transmission, allowing it to maximize fuel economy. Near dynein's stall force, 1 pN, the motor takes 8-nm steps. At <0.4 pN, however, it seems to advance in larger increments of 24 or 32 nm. Thus, dynein can apparently shift into high gear when carrying a light load. Assuming that the coupling ratio under both conditions is equal, the larger step size will result in proportionally better fuel economy.

2.11
Walk This Way: Processive Mechanoenzymes Move Hand-over-hand

The fact that single kinesin molecules generate hundreds of steps, even under load, together with the earlier findings of motion parallel to the protofilaments and

the requirement for two heads, suggested that it might walk – or waddle – from one tubulin dimer to the next. An attractive hypothesis was that the twin heads each take turns, alternately detaching and moving past one another, in a "hand-over-hand" motion resembling that of a person swinging along monkey bars. The same model was also thought to apply to the processive myosin-family motor, myosin V.

Single molecule experiments with myosin V and kinesin have confirmed that both walk hand-over-hand. First, the stride length of myosin V was measured by labeling one of its two heads with a fluorophore, and tracking the label with nanometer resolution. This is like watching a person walking across a field on a moonless night with a flashlight attached to one foot: The person is invisible, but the light moves visibly with every other step. The heads of myosin V took turns making strides that were twice as long as the distance moved by the tail, evidence that strongly supported a hand-over-hand model. Next, optical trapping experiments showed that some kinesin molecules limp along the microtubule, exhibiting a difference in the timing of every other step. Limping implied that kinesin switched between two different configurations as it stepped. The most severe limpers were mutants in which one head hydrolyzed ATP more slowly than the other, arguing for a mechanism in which the two heads swap both mechanical and catalytic activities with each step. Finally, the stride length for one of kinesin's two heads was measured to be 16 nm, double the step size. Taken together, these results make a very strong case for a hand-over-hand mechanism for kinesin and myosin V.

2.12 Coordination is Required

To fully account for the hand-over-hand walking of kinesin and myosin V, coordination between the two heads is essential, and it may be achieved through mechanical tension between the heads. The mechanical cycle of both motors includes a transient state in which both heads are attached to the filament. The motors are probably stretched in this doubly attached state, owing to the relatively large distance between the heads, and the resulting intermolecular strain between the heads could bias their kinetics so that the trailing head nearly always detaches before the leading head. In support of this hypothesis, external loads have been shown to strongly affect the rate of detachment of single myosin V heads, with forward loads accelerating detachment and backward loads slowing detachment.

Coordinated action at distinct sites is a universal requirement for all motors, not just those with high processivity. Automobile engines rely on the carefully timed actions of pistons, valves, and spark plugs. Mechanoenzymes also have critical interacting parts. Consider the mechanochemical cycle of myosin: Within a few milliseconds after attachment of a myosin head to actin, small motions occur in the nucleotide-binding pocket, allowing phosphate release. This triggers lever-arm tilting, which moves the actin filament. Subsequent ADP release triggers a second, smaller motion in certain myosin types (e.g. myosin I and single myosin V heads), but it is not clear if this additional stroke occurs for muscle myosin. ATP binding triggers detachment from actin, and hydrolysis "primes" the motor for the next cycle. For other motors, the specifics and timing are different than for myosin,

but this coordinated action is a universal requirement.

2.13 The Kinesin Cycle and Working Stroke

The mechanochemical cycle of kinesin is not as thoroughly understood as that of myosin. Because two heads are involved in the stepping process, the kinesin cycle is necessarily more complex than that of muscle myosin. The specific conformational changes driving motion are poorly defined, and there is uncertainty about which biochemical events are associated with motion. A working hypothesis for kinesin is that all the mechanical action is associated with just one biochemical event. In support of this "one-stroke" hypothesis, reaction schemes with just one force-dependent rate can account for force-velocity and [ATP]-velocity curves measured in single molecule assays. These schemes predict a working stroke after ATP binding, possibly upon ATP hydrolysis. By contrast, a working stroke concomitant with ATP binding is suggested by kinetic measurements, showing that ADP release from one head is stimulated by binding of a nonhydrolyzable ATP analog (e.g. AMPPNP) to the other head.

A conformational change in the structure of kinesin has been discovered that may drive its motion. This putative working stroke is quite different from either the tilting lever-arm of myosin, or the stem reorientation of dynein. In single-headed kinesin constructs, a 15-amino acid peptide known as the "neck linker," which connects each kinesin head to the coiled-coil stalk, undergoes a nucleotide-dependent transition. In the presence of ADP, or when no nucleotide is present, the neck linker is disordered. In this state, it acts like a flexible tether, pivoting about a point on the backside of the head. When the head is attached to a microtubule in the presence of ATP analogs (AMPPNP, ADP-AlF_4^-), the neck linker "zips" onto to the surface of the head, and its end points toward the microtubule plus end. In the full two-headed motor, zipping of the neck linker on one head could drive stepping by moving the stalk, and therefore the other head, toward the next attachment site on the microtubule lattice.

2.14 Under the Hood, Motors are Still a Mystery

Even for the best-understood motors, where high-resolution structures are available, and major mechanical steps can be identified with specific biochemical transitions, there are very fundamental questions that remain unanswered. In particular, the atomic-scale motions that transduce small chemical events in the nucleotide pocket and convert them into larger motions elsewhere are poorly understood. Important residues have been identified by comparing sequences of related motors and their precursors (e.g. myosin, kinesin, and G-proteins), and subdomains that move relative to others have been suggested by structural comparison. However, ultimately, these static structures cannot elucidate the timing of movements and the cause-and-effect relationships between the various parts. A myriad of physical and biological techniques will no doubt be essential in this effort, but single molecule techniques that simultaneously record motion and biochemical changes (e.g. through fluorescence) seem particularly valuable in this regard.

3
Nontraditional Molecular Motors

There are many other protein machines that generate force and motion, but which do not fit the classic motor paradigm. A growing number are being studied using *in vitro* assays, like those discussed above, which allow the mechanical output of single motors to be measured.

3.1
Nucleic Acid Enzymes

Some of the most important processes of life are carried out by nucleic acid enzymes, many of which are processive motors that move along DNA. Every human cell stores genetic information in the form of 23 strands of DNA, totaling three billion base pairs, and measuring 1 m in total length. All 23 strands are copied by DNA polymerase enzymes, untangled by topoisomerase enzymes, and packaged into chromosomes by condensins, before cell division. The genetic information contained in the DNA is transcribed into mRNA by RNA polymerase (RNAP), and translated into protein by the ribosome. Each of these nucleic acid enzymes is a protein machine capable of generating force and motion, and each is fascinating in its own right. A discussion of all of them is beyond the scope of this chapter, which will focus on one important example, RNAP.

3.2
More Than a Motor: Multitasking by RNA Polymerase

Even though the size of an RNAP enzyme, by comparison of total molecular weight, is not so different from that of the classic mechanoenzymes, its function is much more complex. Motion is merely a by-product of the biological role of this protein machine, transcribing the genetic code. While moving along a DNA template, RNAP separates a short section of the DNA duplex, the "transcription bubble," and builds a copy of one strand by selecting complementary nucleotides from the surrounding solution and attaching them, one at a time, to the end of the nascent mRNA chain (Fig. 1d). Along the way, it must maintain registration of a short section of "hybrid" RNA:DNA duplex, and also respond to a number of different signals that control the initiation, termination, and elongation rate of transcription. Like other mechanoenzymes, RNAP derives energy from nucleotide hydrolysis, but, in this case, each nucleotide serves a dual role. After hydrolysis, the nucleotide becomes an information-containing subunit incorporated into the growing mRNA. (If automobile engines could make such efficient use of their exhaust, urban air quality would be much improved!)

Motion may not be its primary function, but RNAP is no slouch of a motor. Its motion can be directly observed by attaching a micron-sized bead, and recording bead motion as the enzyme transcribes a DNA template bound at one end to a glass surface (Fig. 2c). Using this "tethered particle" assay in conjunction with optical trapping, the motion of a single RNAP can be tracked with high spatial resolution, and the effect of applied load can be measured. RNAP is slow, moving in these assays at 10 to 15 bp s^{-1}, or just 5 nm s^{-1} (Table 1). This speed is roughly equivalent to the rate of human hair growth, and 160-fold slower than the speed of kinesin. However, RNAP is much more processive than kinesin. In cells, RNAP molecules synthesize mRNA chains of 10^4 (in

bacteria) to 10^6 (in mammals) nucleotides. *In vitro*, its processivity is reduced, but the enzyme typically moves across several thousand bases or more before detaching from the template. Movement continues, unhindered at 10 to 15 bp s^{-1}, even when backward loads as high as 27 pN are applied. A high stall force (>5-fold higher than that of kinesin) may be necessary for RNAP to function *in vivo*, perhaps allowing the enzyme to push through "road-blocks" formed by other DNA-binding proteins. RNAP is presumed to move in discrete steps corresponding to the distance between individual bases along the DNA helix, 0.34 nm. This distance is extraordinarily small (20 times smaller than kinesin's 8-nm steps), and steps of this size have not yet been directly observed. However, optical trapping technology is rapidly advancing, and such tiny motions may soon be resolvable.

3.3
RNA Polymerase Structure

RNAP is shaped like a claw. The claw opens to allow a DNA strand to enter, and during transcription it closes, wrapping completely around the DNA. Besides the DNA entry and exit channels, there is also a channel through which the newly synthesized RNA exits, and a pore for nucleotide entry (Fig. 1d). Inside the closed structure, the enzyme makes numerous contacts with the hybrid duplex and the DNA. It is unknown, which parts of RNAP are responsible for generating motion and force production, but many candidate features are apparent in the high-resolution structures. For example, a "bridge helix" located near the site of nucleotide addition may undergo a conformational change that pushes the enzyme to the next site. Determining which portions of RNAP are responsible for its motion is a great challenge for future research.

3.4
What Causes Pauses?

The motion of RNAP along the DNA template is interrupted by pauses, lasting from a few seconds to many minutes. The short-duration pauses (those with lifetimes of seconds) are very frequent, and may result from the enzyme encountering a few GC-rich base pairs of DNA that are tougher-than-average to separate. Occasionally, the enzyme pauses for a much longer duration (20 s to >30 min). These infrequent but long-lived pauses may occur for two reasons, both of which illustrate the sophisticated behavior that RNAP is capable of. First, long pauses can be induced when RNAP encounters a specific sequence in the DNA template it is transcribing. Such sequence-dependent pauses are an important mechanism for regulation of gene expression. By relieving these long pauses, a cell can greatly alter the rate of expression of a pause-containing gene. In some cases, these sequence-dependent pauses occur when the nascent mRNA chain folds into a hairpin structure, which then interacts directly with the RNAP enzyme. In other cases, these pauses occur when the RNAP transcribes a slippery AT-rich sequence, resulting in an unstable RNA:DNA hybrid duplex that allows the enzyme to backtrack. There is a second class of long-duration pauses that are not sequence-dependent, and these probably occur when the enzyme makes a copying error, misincorporating a noncomplementary nucleotide into the mRNA chain. These pauses are also associated with backtracking, and may reflect a

"proofreading" activity whereby the enzyme slides backward and then (with the help of accessory factors) cleaves a short section from the end of the mRNA, removing the mistake before resuming elongation. Determining the reasons why RNAP pauses is critical for understanding how gene transcription is controlled. Single molecule experiments will be useful in this effort because the motion of unsynchronized molecules can be followed with very high resolution, in real time.

3.5 ATP Synthase

A rotary machine, F_1F_0-ATP synthase, is at the heart of energy metabolism in plants, animals, and photosynthetic bacteria, where its role is to replenish the cellular store of ATP. The importance of this job is obvious when one considers that a human body contains 100 g of ATP (0.25 moles), each molecule of which gets hydrolyzed 400 times a day to power various cellular tasks. An army of ATP synthase enzymes performs the $\sim 10^{26}$ synthesis reactions required to regenerate the spent ATP. To do so, the enzymes tap into an electrochemical gradient, the protonmotive force, that exists across the inner mitochondrial membrane of animal cells, or across the thylakoid and plasma membranes of plants and eubacteria, respectively.

ATP synthase consists of two separate rotary motors, F_0 and F_1, that work together as a motor–generator pair. Normally, F_0 is the driving motor of the pair. As protons flow through it, down the electrochemical gradient, a portion of F_0 spins like a water wheel. The spinning wheel of F_0 supplies torque that rotates a shaft within the other motor, F_1, causing it to regenerate ATP from ADP and phosphate. The motor–generator pair can also operate in reverse. In this case, ATP hydrolysis by the F_1 motor causes the shaft to rotate backward, which supplies a torque that spins the wheel of F_0 and pumps protons back up the electrochemical gradient.

F_1F_0-ATP synthase is comprised of eight different types of protein subunits (Fig. 1e). The water wheel, or "rotor" portion of F_0 is a ring of 12 identical subunits, c_{12}, that spin in the plane of the membrane relative to a "stator" composed of three other subunits, ab_2. F_1, is a donut-shaped structure made of three pairs of proteins, $(\alpha\beta)_3$, plus two additional proteins, γ and ε, which form the shaft that fits into the center of the donut. Clockwise (CW) rotation of the $\gamma\varepsilon$ shaft (as seen from the F_0 or membrane side) causes ATP synthesis to occur sequentially at three catalytic sites located symmetrically around the $(\alpha\beta)_3$ ring. Because isolated F_1 can function in reverse, catalyzing ATP hydrolysis and counter clockwise (CCW) rotation of the shaft, it is often referred to as F_1-ATPase. In the full, F_1F_0-ATP synthase enzyme, F_1 sits directly above F_0, with the $\gamma\varepsilon$ shaft of F_1 making a rigid connection to the c_{12} ring of F_0, and with the ab_2 stator of F_0 connecting to the $(\alpha\beta)_3$ donut of F_1. Normally, spinning of c_{12} drives rotation of $\gamma\varepsilon$ within $(\alpha\beta)_3$ and hence ATP synthesis.

The ring-shaped structures within F_1F_0-ATP synthase provided the first clues that rotation might be important to its function. As for the classic mechanoenzymes, proof of motion came when an *in vitro* assay was developed, allowing the rotation to be directly observed. F_1-ATPase molecules were attached sparsely to a surface, and the orientations of their $\gamma\varepsilon$ shafts were marked by attaching micron-long, fluorescent-labeled actin filaments. In the presence of ATP, the filaments rotated CCW, indicating shaft rotation. At very

low concentrations of ATP, the filaments rotated in discrete steps, dwelling at well-defined orientations in between rapid, 120° reorientations. Rotation rates were one-third of the rate of ATP hydrolysis, implying that each 120° reorientation corresponds to hydrolysis of a single ATP. The filaments used to mark shaft orientation also supplied a drag force acting against the rotation. By calculating the drag on the filaments, F_1 was estimated to deliver 40 pN nm of torque during each 120° reorientation, giving 80 pN nm of mechanical work output per ATP hydrolysis. This is 100% of the available chemical energy, making F_1-ATPase one of the most efficient motors known.

F_1-ATPase is a relative newcomer to the molecular motor scene, but it is quickly becoming one of the best-understood examples of mechanochemical coupling. A series of experiments with single F_1 molecules has revealed that each 120° step occurs in two phases, or substeps, that correspond to particular biochemical transitions in the ATP synthesis reactions occurring at each of the three catalytic sites. Substeps were observed by marking the shaft orientation with 40-nm gold particles (Fig. 2d), rather than the much larger filaments used in earlier work. The small beads resulted in a lower drag force acting on the motor, allowing full speed rotation at 160 revolutions per second (Hz) (Table 1). Capturing the motion with a high-speed video camera showed a substep of 80 to 90° followed by one of 30 to 40°, underlying each of the 120° steps previously observed. Finally, simultaneous observation of shaft orientation and binding and release of a fluorescent nucleotide allowed these biochemical steps to be temporally correlated with the substeps. ATP binding to one of the catalytic sites (site 0) is concurrent with the 80 to 90° substep, and the remaining 30 to 40° substep requires hydrolysis at the site that previously bound ATP (site −1), and release of ADP from the remaining site (−2).

It is unknown whether the events seen during ATP hydrolysis by F_1 are simply the reverse of those occurring during synthesis, but several experiments confirm, at least, that the $\gamma\varepsilon$ shaft rotates in the opposite direction during synthesis. In one experiment, magnetic beads attached to the shaft were used to drive CW rotation in F_1-ATPase, in the presence of ADP and phosphate, and a luciferin–luciferase system that emits a photon upon reacting with ATP was used to verify synthesis. In another experiment, individual, fluorescent-labeled F_1F_0-ATP synthase complexes were embedded in liposomes. A pH difference was created across the membrane by rapid dilution, and rotation was recorded by fluorescence resonance energy transfer (FRET).

3.6 The Rotary Motor of Bacterial Flagella

Bacterial flagella are very different from the flagella and cilia of eukaryotic cells. Flagellated bacteria, such as *Escherichia coli*, swim by rotating a set of four corkscrew-shaped filaments (four, on average) that extend from the cell surface out into the surrounding medium. At the base of each filament is a large protein machine that drives filament rotation. This rotary motor, like F_1F_0-ATP synthase, is powered by the protonmotive force, but it is much larger and structurally more complex than F_1F_0-ATP synthase.

Bacteria swim to find food. They control their swimming behavior by altering the direction of rotation of their flagellar motors. When all four motors rotate CCW

(as seen by an observer outside the cell), the cell swims steadily, or "runs," in a relatively straight line parallel to its long axis. When one or more motors rotates CW, the cell "tumbles," erratically moving in place and reorienting itself. The motors switch from CCW to CW at random, so that typical swimming involves runs that last ~1 s, interspersed with tumbles that last a few milliseconds. When the bacteria senses rising nutrient concentrations, it lengthens the runs by increasing the probability of CCW rotation. In this way, the cell moves, on average, toward the food.

The core of the bacterial flagellar motor is a stack of ring-shaped structures, 45 nm in diameter, embedded in the multilayered cell envelope (see Fig 1f). The rings are composed of 20 different types of proteins, but they are all thought to rotate together as a single unit, the "rotor." Rotation of the stack of rings is driven by a circular array of $\leq$16 "studs" that surround the base of the stack, and which are anchored to the framework of the cell wall. Each stud is composed of two MotA proteins (32 kDa), and one MotB protein (34 kDa). No high-resolution structures are available for the MotA/MotB complex, but both proteins span the cytoplasmic membrane, forming a transmembrane proton channel. MotB has a proton-acceptor site, and MotA contains a site that interacts with the base of the rotor. Protonation and deprotonation of MotB is thought to cause conformational changes in MotA, which probably binds and unbinds from the rotor, driving rotation and torque generation. The minimal torque-generating unit may be composed of two studs (i.e. four MotA subunits plus two MotB subunits). More detailed descriptions of the structure can be found in review articles cited in the bibliography.

Individual flagellar motors can be studied by attaching bacteria to a glass surface by one flagellum. The tail wags the dog in this tethered cell assay – with the flagellum anchored, rotation of the motor causes the whole cell body to spin. To spin the entire cell, the motor must overcome a large viscous drag, so it spins relatively slowly in this assay, at 10 Hz. But it produces an impressive 4600 pN nm of torque. When mutant cells lacking MotB are tethered, they are paralyzed and do not spin. Amazingly, these paralyzed cells can be "resurrected" by expression of MotB from an inducible gene. Resurrected cells begin to rotate within several minutes after induction of MotB expression, and their speed increases in a series of discrete jumps. Each jump in speed represents the incorporation of one additional torque-generating unit into the motor. As many as eight jumps can be seen, implying that the maximum number of torque generators is eight.

Each torque generator is itself a processive, high-duty ratio motor that moves along the surface of the rotor without detaching. The best evidence for processivity is that tethered cells in the resurrection experiment with just one torque-generating unit spin relatively smoothly, and do not freely undergo rotational Brownian motion. Evidently, a single unit is sufficient to prevent the motor from slipping, and each unit remains attached to the rotor during most, or all, of its mechanical cycle. There are twice as many studs (16) as torque-generating units (8), and one hypothesis is that each unit is a coordinated pair of studs, possibly moving in a hand-over-hand motion like that of

kinesin or myosin V. A single unit is expected to move stepwise over the surface of the rotor, perhaps taking ~26 steps per revolution (the approximate number of subunits composing the base of the rotor), but such steps have not been directly observed. Dividing the maximum torque (4600 pN) by the number of torque-generating units (8), and by their distance from the axis of rotation (20 nm), shows that each unit generates considerable force, up to 29 pN, which is comparable to the stall force of RNAP. Their speed of motion over the rotor surface is also quite high. When the viscous load is minimal, the motor can rotate as fast as 300 Hz (Table 1). This translates into motion of the torque-generators at 38 000 nm s^{-1} over the rotor surface, which is >6-fold faster than muscle myosin, and similar to the speed of the fastest myosins (e.g. type XI, responsible for cytoplasmic streaming in algae).

The speed of rotation is proportional to the protonmotive force, as shown by wiring a cell to an external voltage source and watching an inert marker on the motor. To apply voltage, the cell body was drawn halfway into a micropipette, and the membrane permeabilized by chemical treatment. Estimates of the proton flux through the motor suggest that the motor is tightly coupled. Roughly 1200 protons flow through the motor during each complete revolution. By attaching a variety of different-sized latex beads to the filaments and adjusting the viscosity of the surrounding fluid, torque-speed relations have been measured over a wide range of speeds. Forward rotation under assisting torques, and backward rotation under torques above stall (>4600 pN), has been explored by using rotating electric fields or optical traps to apply torque in the tethered cell assay.

3.7 Polymers that Push and Pull

Actin filaments and microtubules are not just static polymers. In addition to their roles as structural cables and girders for maintaining cell shape, and as superhighways for mechanoenzymes to move along, these polymers are also dynamic machines that can produce force. In living cells, the cytoskeletal polymers are in a constant state of flux, and their growth and shrinkage is harnessed to drive many organelle and whole-cell movements. Crawling cells have a dense array of polymerizing actin filaments beneath their leading edge that pushes outward on the plasma membrane and causes protrusion. Similarly, the bacterial pathogen, *Listeria monocytogenes* is pushed by actin polymerization. The bacteria move in graceful arcs through the cytoplasm of a host cell, leaving "comet tails" of polymerized actin in their wake. During mitosis, chromosomes are pushed and pulled by dynamic microtubules whose ends are linked to specialized sites on the chromosomes, the kinetochores. Just before cell division, kinetochore-attached microtubules depolymerize, generating tension that pulls sister chromatids apart.

Both actin and microtubule filaments are composed of protein subunits arranged in a regular lattice. The monomeric form of actin, "G-actin," is a roughly spherical protein, 5 nm in diameter (45 kDa). Like a LEGO block, the surface of an actin monomer has several sites for attachment to other monomers. Each also has a cleft that binds an ATP molecule. Monomers assemble into a ropelike structure, "F-actin," with two strands, called *protofilaments*, that wind around each other with a helical period of 72 nm. The building blocks for microtubules are made

of tubulin, a molecule that consists of two nearly identical 50-kDa proteins fused tightly to form a dimer, 8 nm in length. Each dimer has two sites that bind GTP. The dimers assemble into a hollow, tube-shaped structure, 25 nm in diameter, with 13 protofilaments that run parallel to the long axis of the tube. Both types of filaments have fast-growing "plus" ends, and slow-growing "minus" ends.

Nucleotide hydrolysis supplies energy that makes actin and tubulin polymers very dynamic. Actin monomers in solution bind ATP, and have high affinity for one another. After polymerization, the ATP is hydrolyzed and phosphate is released, leaving ADP trapped in the binding clefts of the monomers within a filament. The ADP-containing monomers have reduced affinity, so hydrolysis destabilizes the actin filament, promoting depolymerization. GTP hydrolysis by tubulin has a similar effect. Each tubulin dimer binds two molecules of GTP, one of which is hydrolyzed upon incorporation of the dimer into a microtubule filament. The GDP-containing tubulin dimers have reduced affinity for one another, which destabilizes the lattice and promotes depolymerization. Without hydrolysis, both polymers would simply grow until equilibrium was reached, when the subunit pool was spent. Hydrolysis keeps the filaments out of equilibrium, allowing coexistence of growing and depolymerizing filaments.

3.8 Microtubule Ends and Dynamic Instability

The dynamic behavior of microtubules can be directly observed *in vitro*. In the presence of GTP and pure tubulin, microtubule growth is interrupted by periods of rapid depolymerization. This "dynamic instability" requires GTP hydrolysis. Growth rates are normal in the presence of the nonhydrolyzable GTP analog, GMPCPP, but the growth is uninterrupted. Subunit addition and removal occurs only at the ends of the filaments, which adopt different structures, depending on whether they are in a state of growth or depolymerization. The protofilaments that extend from growing ends are straight, forming sheets that are sometimes hundreds of subunits long. In contrast, the protofilaments at depolymerizing ends become highly curved, peeling away from the lattice. The ends of growing filaments are temporarily stabilized by a "cap" of GTP-containing subunits in which hydrolysis has not yet taken place. The transition between growth and depolymerization, called "catastrophe," is probably triggered when hydrolysis of the cap occurs before more GTP-containing subunits are added.

The curvature of protofilaments at the ends of depolymerizing microtubules, and the fact that the products of depolymerization are often curved oligomers, suggests a structural basis for the coupling of nucleotide hydrolysis and polymerization. Before hydrolysis, the GTP-containing dimers are probably straight, fitting snugly into the growing microtubule lattice. If the GDP-containing subunits are naturally curved, then they would be strained when trapped within the lattice. In this way, energy from hydrolysis could be stored within the lattice as mechanical strain.

3.9 Motility Assays with Cytoskeletal Filaments

Several *in vitro* experiments show that polymerization of pure actin or tubulin, without any additional proteins, can generate pushing force and do mechanical work. Polymerizing actin filaments inside

liposomes causes distension of the liposomes, demonstrating that the growing filaments can push outward on the lipid bilayer. Likewise, microtubule filaments grown inside a small chamber can push against the chamber walls with enough force to buckle themselves (Fig. 1e). By analyzing the shapes of buckled filaments, the maximum pushing force of a single microtubule has been estimated at 4 pN.

These important experiments prove that growing filaments can push against an object, but they are incomplete models for the polymer-driven motility that occurs in cells. In cells, a variety of accessory proteins provide spatial and temporal control of filament dynamics, and couple the ends of growing and shrinking filaments to other structures to apply force. *Listeria* promote spatially localized actin polymerization with a nucleation factor, ActA. Likewise, kinetochores contain a host of proteins that modulate microtubule dynamics and maintain attachment to microtubule ends. Understanding the mechanisms of these accessory factors will be key to understanding how cells harness cytoskeletal filaments to produce motion and force.

In vitro motility assays that reconstitute force generation using dynamic filaments coupled to accessory proteins provide more realistic models for filament-based motility in cells. Shrinking microtubules can pull against microscopic beads when the beads are coated with proteins that maintain attachment to the depolymerizing filament ends. This motion is similar to the way chromosomes are pulled apart before cell division, and also to the way the mitotic spindle is positioned inside asymmetrically dividing yeast cells. In a reconstituted assay that closely mimics the motion of *Listeria*, beads coated with ActA protein are pushed around by actin polymerization. The beads follow curved trajectories and leave comet tails of polymerized actin in their wake, just like the bacteria.

4 Conclusion

Motion is fundamental to life. Everyone is familiar with the macroscopic motion of muscle contraction. There are also exquisite motions taking place at the level of cells and molecules. The cells in our immune system crawl around our bodies and engulf invading bacteria. Cilia in our lungs beat to remove inhaled debris. In all these cases, the motion is generated by tiny protein machines, the molecular motors. Molecular motors are ubiquitous, and the list of known motors is growing. Besides the classic motors, myosin, kinesin, and dynein, and the cytoskeletal polymers, filamentous actin and microtubules, there are also protein machines at the heart of energy metabolism, and reading the genetic code. Studies of molecular motors, particularly *in vitro* work with single molecules, have revealed fascinating details about how they convert chemical energy into mechanical work.

While motors are arguably the most machinelike of the biological molecules, they are certainly not the only things inside living cells that remind us of man-made apparatus. The action at a distance that occurs within an allosteric enzyme, for example, is reminiscent of the push rods or levers inside an internal combustion engine. The large, multienzyme complexes that cells use to carry out sequences of reactions remind us of assembly lines. However, molecular

motors are an important special case because the motions they produce are large enough to be directly measured. The study of motor proteins offers rare, direct access to address general questions about how a protein's structure dictates it's dynamics and function.

See also Nucleic Acid and Protein Single Molecule Detection and Characterization.

Bibliography

Books and Reviews

Berg, H.C. (2003) The rotary motor of bacterial flagella, *Annu. Rev. Biochem.* **72**, 19–54.

Block, S.M. (1995) Nanometres and piconewtons: the macromolecular mechanics of kinesin, *Trends Cell Biol.* **5**, 169–175.

Cameron, L.A., Giardini, P.A., Soo, F.S., Theriot, J.A. (2000) Secrets of actin-based motility revealed by a bacterial pathogen, *Nat. Rev. Mol. Cell Biol.* **1**, 110–119.

Howard, J. (2001) *Mechanics of Motor Proteins and the Cytoskeleton*, Sinauer Associates, Publishers, Sunderland, MA.

Inoue, S., Salmon, E.D. (1995) Force generation by microtubule assembly/disassembly in mitosis and related movements, *Mol. Biol. Cell* **6**, 1619–1640.

Salmon, E.D. (1995) VE-DIC light microscopy and the discovery of kinesin, *Trends Cell Biol.* **5**, 154–158.

Schliwa, M. (2003) *Molecular Motors*, Wiley-VCH, Weinheim.

Schliwa, M., Woehlke, G. (2003) Molecular motors, *Nature* **422**, 759–765.

Spudich, J.A. (2001) The myosin swinging cross-bridge model, *Nat. Rev. Mol. Cell Biol.* **2**, 387–392.

Vale, R.D., Milligan, R.A. (2000) The way things move: looking under the hood of molecular motor proteins, *Science* **288**, 88–95.

Yoshida, M., Muneyuki, E., Hisabori, T. (2001) ATP synthase–a marvellous rotary engine of the cell, *Nat. Rev. Mol. Cell Biol.* **2**, 669–677.

Primary Literature

Asbury, C.L., Fehr, A.N., Block, S.M. (2003) Kinesin moves by an asymmetric hand-over-hand mechanism, *Science* **302**, 2130–2134.

Berliner, E., Young, E.C., Anderson, K., Mahtani, H.K., Gelles, J. (1995) Failure of a single-headed kinesin to track parallel to microtubule protofilaments, *Nature* **373**, 718–721.

Block, S.M., Berg, H.C. (1984) Successive incorporation of force-generating units in the bacterial rotary motor, *Nature* **309**, 470–472.

Burgess, S.A., Walker, M.L., Sakakibara, H., Knight, P.J., Oiwa, K. (2003) Dynein structure and power stroke, *Nature* **421**, 715–718.

Case, R.B., Pierce, D.W., Hom-Booher, N., Hart, C.L., Vale, R.D. (1997) The directional preference of kinesin motors is specified by an element outside of the motor catalytic domain, *Cell* **90**, 959–966.

Diez, M., Zimmermann, B., Borsch, M., Konig, M., Schweinberger, E., Steigmiller, S., Reuter, R., Felekyan, S., Kudryavtsev, V., Seidel, C.A., Graber, P. (2004) Proton-powered subunit rotation in single membrane-bound F0F1-ATP synthase, *Nat. Struct. Mol. Biol.* **11**, 135–141.

Dogterom, M., Yurke, B. (1997) Measurement of the force-velocity relation for growing microtubules, *Science* **278**, 856–860.

Finer, J.T., Simmons, R.M., Spudich, J.A. (1994) Single myosin molecule mechanics: piconewton forces and nanometre steps, *Nature* **368**, 113–119.

Hancock, W.O., Howard, J. (1998) Processivity of the motor protein kinesin requires two heads, *J. Cell Biol.* **140**, 1395–1405.

Henningsen, U., Schliwa, M. (1997) Reversal in the direction of movement of a molecular motor, *Nature* **389**, 93–96.

Howard, J., Hudspeth, A.J., Vale, R.D. (1989) Movement of microtubules by single kinesin molecules, *Nature* **342**, 154–158.

Hua, W., Young, E.C., Fleming, M.L., Gelles, J. (1997) Coupling of kinesin steps to ATP hydrolysis, *Nature* **388**, 390–393.

Ishijima, A., Kojima, H., Funatsu, T., Tokunaga, M., Higuchi, H., Tanaka, H., Yanagida, T. (1998) Simultaneous observation of individual ATPase and mechanical events by a single myosin molecule during interaction with actin, *Cell* **92**, 161–171.

Lang, M.J., Fordyce, P.M., Block, S.M. (2003) Combined optical trapping and single-molecule fluorescence, *J. Biol.* **2**, 6.

Lister, I., Schmitz, S., Walker, M., Trinick, J., Buss, F., Veigel, C., Kendrick-Jones, J. (2004) A monomeric myosin VI with a large working stroke, *EMBO J.* **23**, 1729–1738.

Loisel, T.P., Boujemaa, R., Pantaloni, D., Carlier, M.F. (1999) Reconstitution of actin-based motility of Listeria and Shigella using pure proteins, *Nature* **401**, 613–616.

Lombillo, V.A., Stewart, R.J., McIntosh, J.R. (1995) Minus-end-directed motion of kinesin-coated microspheres driven by microtubule depolymerization, *Nature* **373**, 161–164.

Mallik, R., Carter, B.C., Lex, S.A., King, S.J., Gross, S.P. (2004) Cytoplasmic dynein functions as a gear in response to load, *Nature* **427**, 649–652.

Mehta, A.D., Rock, R.S., Rief, M., Spudich, J.A., Mooseker, M.S., Cheney, R.E. (1999) Myosin-V is a processive actin-based motor, *Nature* **400**, 590–593.

Meyhofer, E., Howard, J. (1995) The force generated by a single kinesin molecule against an elastic load, *Proc. Natl. Acad. Sci. U S A* **92**, 574–578.

Nishizaka, T., Oiwa, K., Noji, H., Kimura, S., Muneyuki, E., Yoshida, M., Kinosita, K. Jr. (2004) Chemomechanical coupling in F1-ATPase revealed by simultaneous observation of nucleotide kinetics and rotation, *Nat. Struct. Mol. Biol.* **11**, 142–148.

Noji, H., Yasuda, R., Yoshida, M., Kinosita, K. Jr. (1997) Direct observation of the rotation of F1-ATPase, *Nature* **386**, 299–302.

Ray, S., Meyhofer, E., Milligan, R.A., Howard, J. (1993) Kinesin follows the microtubule's protofilament axis, *J. Cell Biol.* **121**, 1083–1093.

Rice, S., Lin, A.W., Safer, D., Hart, C.L., Naber, N., Carragher, B.O., Cain, S.M., Pechatnikova, E., Wilson-Kubalek, E.M., Whittaker, M., Pate, E., Cooke, R., Taylor, E.W., Milligan, R.A., Vale, R.D. (1999) A structural change in the kinesin motor protein that drives motility, *Nature* **402**, 778–784.

Ryu, W.S., Berry, R.M., Berg, H.C. (2000) Torque-generating units of the flagellar motor of Escherichia coli have a high duty ratio, *Nature* **403**, 444–447.

Sakakibara, H., Kojima, H., Sakai, Y., Katayama, E., Oiwa, K. (1999) Inner-arm dynein c of Chlamydomonas flagella is a single-headed processive motor, *Nature* **400**, 586–590.

Schafer, D.A., Gelles, J., Sheetz, M.P., Landick, R. (1991) Transcription by single molecules of RNA polymerase observed by light microscopy, *Nature* **352**, 444–448.

Schnitzer, M.J., Block, S.M. (1997) Kinesin hydrolyses one ATP per 8-nm step, *Nature* **388**, 386–390.

Shaevitz, J.W., Abbondanzieri, E.A., Landick, R., Block, S.M. (2003) Backtracking by single RNA polymerase molecules observed at near-base-pair resolution, *Nature* **426**, 684–687.

Svoboda, K., Block, S.M. (1994) Force and velocity measured for single kinesin molecules, *Cell* **77**, 773–784.

Svoboda, K., Schmidt, C.F., Schnapp, B.J., Block, S.M. (1993) Direct observation of kinesin stepping by optical trapping interferometry, *Nature* **365**, 721–727.

Vale, R.D., Reese, T.S., Sheetz, M.P. (1985) Identification of a novel force-generating protein, kinesin, involved in microtubule-based motility, *Cell* **42**, 39–50.

Vale, R.D., Funatsu, T., Pierce, D.W., Romberg, L., Harada, Y., Yanagida, T. (1996) Direct observation of single kinesin molecules moving along microtubules, *Nature* **380**, 451–453.

Veigel, C., Wang, F., Bartoo, M.L., Sellers, J.R., Molloy, J.E. (2002) The gated gait of the processive molecular motor, myosin V, *Nat. Cell Biol.* **4**, 59–65.

Yasuda, R., Noji, H., Kinosita, K. Jr., Yoshida, M. (1998) F1-ATPase is a highly efficient molecular motor that rotates with discrete 120 degree steps, *Cell* **93**, 1117–1124.

Yasuda, R., Noji, H., Yoshida, M., Kinosita, K. Jr., Itoh, H. (2001) Resolution of distinct rotational substeps by submillisecond kinetic analysis of F1-ATPase, *Nature* **410**, 898–904.

Yildiz, A., Tomishige, M., Vale, R.D., Selvin, P.R. (2004) Kinesin walks hand-over-hand, *Science* **303**, 676–678.

Yildiz, A., Forkey, J.N., McKinney, S.A., Ha, T., Goldman, Y.E., Selvin, P.R. (2003) Myosin V walks hand-over-hand: single fluorophore imaging with 1.5-nm localization, *Science* **300**, 2061–2065.

Yin, H., Wang, M.D., Svoboda, K., Landick, R., Block, S.M., Gelles, J. (1995) Transcription against an applied force, *Science* **270**, 1653–1657.